Atmospheric boundary layer adjustment to the synoptic cycle at the Brazil-Malvinas Confluence, South Atlantic Ocean

Otávio C. Acevedo,[1] Luciano P. Pezzi,[2] Ronald B. Souza,[3] Vagner Anabor,[1] and Gervásio A. Degrazia[1]

Received 28 December 2009; revised 25 May 2010; accepted 2 August 2010; published 17 November 2010.

[1] This study analyzes and discusses atmospheric boundary layer vertical profiles of potential temperature, specific humidity, and wind speed at each of the sides of the Brazil-Malvinas Confluence in the southwestern Atlantic Ocean. Such confluence is characterized by the meeting of water masses with very different characteristics: the southern waters of the Malvinas current can be several degrees colder and appreciably less salty than the northern Brazil current waters. At the same time, a synoptic cycle can be identified at the region, marked by the successive passages of frontal systems and extratropical cyclones. The different phases of the synoptic cycle lead to different thermal advections at the confluence, causing respective different patterns of atmospheric boundary layer adjustment to the surface heterogeneity induced by the confluence. In the present study, this adjustment along the synoptic cycle is analyzed using data from five experiments performed across the confluence from 2003 to 2008. In each of the campaigns a number of soundings were launched from a ship at both sides of the confluence. A climatological analysis with respect to the closest frontal passage is presented, and it suggests that the observations collected at each of the years analyzed are referent to a different day of the synoptic cycle. The average profiles at each side of the confluence are in agreement with previous modeling studies of warm and cold thermal advection patterns over an oceanic front. Furthermore, our study shows that peculiar transitional characteristics are also observed between the conditions of well-established warm and cold advection. At many phases of the synoptic cycle a strongly stratified boundary layer occurs at one or both sides of the confluence. Some of the observed characteristics, such as a large moisture accumulation near the surface, suggest that existing sensible and latent heat fluxes parameterizations fail under very strong stratifications, and the consequences of this deficiency are analyzed.

Citation: Acevedo, O. C., L. P. Pezzi, R. B. Souza, V. Anabor, and G. A. Degrazia (2010), Atmospheric boundary layer adjustment to the synoptic cycle at the Brazil-Malvinas Confluence, South Atlantic Ocean, *J. Geophys. Res.*, *115*, D22107, doi:10.1029/2009JD013785.

1. Introduction

[2] The thermal and saline contrasts between distinct water masses in the ocean are responsible for the generation of oceanographic fronts in both mesoscale and large scale in the World Ocean. At the ocean-atmosphere interface, intense momentum gradients and energy vertical fluxes can be generated in association to the horizontal distribution of the sea surface temperature, SST [*Lindzen and Nigam*, 1987; *Hayes et al.*, 1989; *Polito et al.*, 2001; *Xie*, 2004; *Pezzi et al.*, 2004, 2005, 2009; *Small et al.*, 2008]. At the same time that these fluxes affect the dynamical and thermodynamical structure of the atmosphere, they also affect, for example, the local distribution of water masses, thermocline depth and heat transport in the ocean. In addition to that, the turbulent processes occurring in small spatial and temporal scales may induce variations on the evolution of large-scale processes in both ocean and atmosphere.

[3] The Brazil-Malvinas Confluence (BMC) region (Figure 1) in the South Atlantic Ocean is the western portion of the Subtropical Front [*Peterson and Stramma*, 1991], being characterized by the meeting of two opposing western boundary currents. From the north, Tropical warm and saline waters are transported by the Brazil Current (BC). From the south, cold and less saline Subantarctic waters are transported by the Malvinas (Falkland) Current (MC). These two current systems meet each other at the BMC region

[1]Department of Physics, Federal University of Santa Maria, Santa Maria, Rio Grande do Sul, Brazil.
[2]Earth Observation General Coordination, National Institute for Space Research, São José dos Campos, São Paulo, Brazil.
[3]Southern Regional Center for Space Research, National Institute for Space Research, Santa Maria, Rio Grande do Sul, Brazil.

0148-0227/10/2009JD013785

forming an active and nonsteady meandering frontal region. The BMC is acknowledged as one of the most energetic regions of the World Ocean [*Chelton et al.*, 1990; *Piola and Matano*, 2001]. The mixing of these distinct water masses causes a convergence of the meeting waters producing the South Atlantic Central Water (SACW). The last spreads itself all over the South Atlantic Ocean in subsurface layers.

[4] The seasonal variability and characteristics of the BMC have been studied since *Deacon* [1937] and *Defant* [1941] (cited by *Olson et al.* [1988]). One of the more remarkable features of the BMC region is that the position of the confluence oscillates seasonally, with the BC reaching the southernmost limits in the Austral summer, and the MC achieving its northernmost limits in the wintertime. *Reid et al.* [1977] established the mean location of the BMC in a range from 36°S (Austral winter) to 39°S (Austral summer). The position in which the BC reverses its direction, however, is further south between 40°S and 46°S. After meeting the MC in the BMC region, the BC separates from the shelf break and penetrates the Atlantic Ocean interior, forming a series of large amplitude meanders. *Legeckis and Gordon* [1982] found the variable limit of 38°S to 46°S as the maximum latitude of warm water related to the BC. The variability of this limit was found to be bimonthly and accompanied by intermittent formation of warm-core anticyclonic eddies [*Souza et al.*, 2006].

[5] *Peterson and Stramma* [1991] point out that the BMC oscillations throughout the year depend on the seasonal cycles elsewhere in the South Atlantic. The subtropical atmospheric high-pressure system, for example, moves northward in the winter, intensifying along the way. Furthermore, the South Equatorial Current (SEC) is also strengthened and displaced to the north in the wintertime, and the zero line of the wind stress curl is shifted 5° in latitude north from its mean position in the summer.

[6] *Garzoli and Garraffo* [1989] link the spatial variation of the BMC to the large-scale variability of the winds and of the SEC which feeds the BC. According to *Olson et al.* [1988], the local wind stress curl may also play a role in the position where the BC separates from the coast (position sometimes interpreted as the BMC location). The authors, however, report that the local winds are unlikely to be uniquely responsible for the BMC oscillation. Another alternative proposed by *Olson et al.* [1988] is the variation in the MC forced by variations in the Antarctic Circumpolar Current (ACC) system. Pressure changes in the Subantarctic Front, where the MC is fed by a branch of the ACC, could reach the BMC region by Kelvin waves. Wind induced advective changes in the MC could also link the Antarctic sector with the BMC region.

[7] It is well known that large-scale processes, such as cyclones and frontal systems have direct influence on the meteorological and marine phenomena affecting South America and its coastal regions. In fact, the weather pattern at the BMC is severely influenced by a synoptic cycle, characterized by the successive passage of cold air masses originated from higher latitudes in South America and in the vicinity of the Antarctic Continent. Such large-scale meteorological phenomena modulate the micrometeorological properties of the marine atmospheric boundary layer (MABL), a typical shear-driven boundary layer, with small surface sensible heat fluxes and fairly large horizontal winds. The shear-driven turbulence is characterized by longer relaxation time scales in comparison to that present in buoyancy-driven, convective boundary layers [*Moeng and Sullivan*, 1994]. As a consequence, the boundary layer at marine regions takes a longer time to adjust itself to large-scale forcing, originated from the frontal passages, than it would take if over terrestrial regions.

[8] Two important features that characterize the BMC region make it an ideal site for studying boundary layer air mass modification under the influence of different large-scale forcings. These are (1) the surface heterogeneity, caused by the confluence between the Brazil and Malvinas currents, and (2) the well-defined synoptic cycle that occurs over latitudes where the BMC exists. The MABL structure under the influence of thermal advection induced by oceanic fronts has been addressed in previous studies. The case with cold air advection has been analyzed by *Pyatt et al.* [2005] and *de Szoeke et al.* [2005], using observations in the equatorial region. *Mahrt et al.* [2004] looked at cases influenced by both cold and warm advection, being primarily interested in the internal boundary layer generated in each of the cases, and its impact on the turbulent structure. A number of additional studies have described observations of warm air advection influencing the MABL structure over coastal regions [e.g., *Smedman et al.*, 1995; *Vickers et al.*, 2001; *Vihma and Brummer*, 2002]. From a modeling perspective, *Skyllingstad et al.* [2007] presented detailed simulations of the MABL structure under the influence of both cold and warm thermal advections over an oceanic front. No study has, however, shown observations of the MABL structure along the different portions of a typical synoptic cycle.

[9] Since 2004, the High Latitudes Oceanography Group (GOAL) under the umbrella of the Brazilian Antarctic Program (PROANTAR) leads scientific cruises across the BMC once a year, during the Austral spring, when simultaneous oceanic and atmospheric observations were made onboard of a Brazilian vessel. A total of 6 cruises have been performed to date, from 2004 to 2009, covering different periods within the typical synoptic cycle of the region (Table 1). The observed data collected in the first four cruises (named OP23 to OP26, years 2004–2007, respectively) have been previously studied by *Pezzi et al.* [2005, 2009]. Data from these 4 previous cruises plus the 2008 cruise (denoted here as OP27) are included in the present study, and a synoptic oceanic and atmospheric view from the study region is shown in Figure 1.

[10] The observations taken during OP23 to OP27 cruises comprise an interesting data set to characterize the boundary layer adjustment along different portions of the cycle, including postfrontal, prefrontal and transition periods, characterized by both cold and warm advection. The influence of these synoptic systems in the MABL structure is, therefore, analyzed in the present study, with regard to the different wind regimes and advective patterns induced by them. In section 2 we describe the observations made. Later in section 3, we discuss the typical synoptic cycle that occurs at the BMC region, presenting composite fields with respect to frontal passages. Such composite climatology guides the analysis presented in section 4, where we describe how the MABL properties are affected by the frontal passages. In section 5, the air-sea heat

Table 1. Experiment Names, Period Descriptions, and Associated Days of the Synoptic Cycles

Experiment	Dates	Closest Frontal Passage Day	Condition	Estimated Thermal Advection (°C d^{-1})
OP23	2–3 November 2004	2 November 2004	day 0	−2.1
OP24	27–28 October 2005	25 October 2005	day +2	−5.8
OP25	27–28 October 2006	29 October 2009	day −2	6.3
OP26	16–17 October 2007	17 October 2007	day −1	4.2
OP27[a]	14–15 October 2008	12 October 2008	day +1	−13.0

[a]Cross frontal estimated thermal advection (°C d^{-1}).

fluxes are analyzed. This paper finishes with section 6, which presents our concluding remarks and suggestions for future work.

2. In Situ Data Collection

[11] As part of the Brazilian Antarctic Program (PROANTAR), the Brazilian Navy Oceanographic Support Ship (OSS) *Ary Rongel* departs from Brazil toward Antarctica every year. The position where the BC reverses its direction (BC return flow) at the BMC region was mapped yearly prior to the vessel's departure from the port city of Rio Grande in southern Brazil. The strong surface thermal gradients between the BC and the MC in the region were mapped every year from 2004 to 2008 with the help of satellite imagery. These maps were used to guide the ship toward the region of maximum horizontal thermal gradients between the BC and the MC (BC/MC front).

[12] Although detailed information about the study area, data description and the sampling strategy can be found in more details in the work of *Pezzi et al.* [2009], the main features are briefly highlighted here. The experiments area is located between 30°S to 50°S, 50°W to 60°W (Figure 1). This area was covered during specific dates in 2004 to 2008 as indicated in Table 1. While crossing the BC/MC front, Expendable Bathy-Thermographs (XBTs) were launched from the OSS *Ary Rongel* in order to measure the water temperature as a function of depth along the ship's route. When at the close vicinity of the front, a sequence of radiosondes was also launched from the rear deck of the ship. The radiosondes measured pressure, temperature and relative humidity (RH) in the atmosphere. Wind speed and direction were also estimated from the relative movement of the radiosonde balloon in the atmosphere. Sampling was made at regular intervals of 2 s, which guaranteed a fair number of observations within the MABL. The radiosonde balloon position was traced with the help of a Global Position System (GPS) device connected to a receptor on board.

[13] The radiosondes were launched when the ship was crossing over from the BC (warm water) to the BC/MC front and to the MC (cold water), launching as many radiosondes were possible in a period of up to 1 day. *Pezzi et al.* [2009] presented spatial and temporal coordinates of each launch. The XBTs were launched simultaneously with the radiosondes or in distances close to a quarter degree latitude. In situ independent meteorological measurements were also made by the ship's meteorological station.

[14] Figure 1 presents the satellite-measured synoptic condition of the SST and near-surface winds in 15 October 2008 (OP27) at the study region. The SST image is derived from the AMSR-E (Advanced Microwave Scanning Radiometer) sensor. Quasi-simultaneous wind data were obtained from the QuikScat sensor. The BC/MC front is clearly noticeable from the large thermal contrasts. As seen in the work of *Pezzi et al.* [2009] for the other experiments, wind vectors are also adjusted to the synoptic SST field in OP27. Wind speed minima are observed over the cold waters of the MC core. Winds are remarkably stronger away from the MC

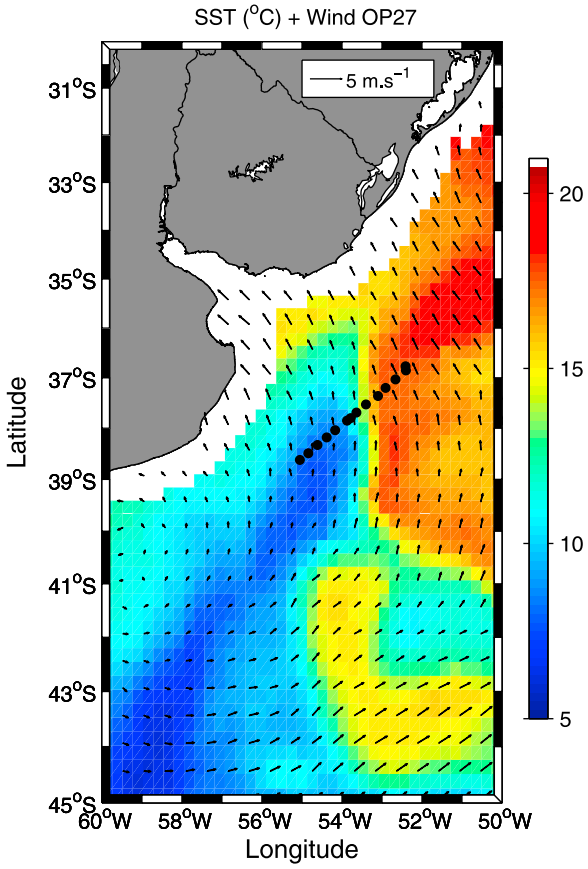

Figure 1. Brazil-Malvinas Confluence study region with radiosonde ascent positions (black circles) denoting the cruise route for OP27. QuikScat wind directions (m s^{-1}) are the vectors superimposed onto AMSR-E SST images. All satellite data are for 15 October 2008 coincident in time with the experiments. The color bar denotes SST in degrees Celsius.

core in coastal and offshore waters and over the BC warm waters. The synoptic pattern of wind adjustment to the sea surface temperature seen in OP27 agrees with previous experiments shown in the work of *Pezzi et al.* [2005, 2009] and the annual climatology presented by *Tokinaga et al.* [2005] for the BMC region. Figure 1 also presents the radiosonde launching positions during OP27. From these positions, the cruise route in the study region can be inferred.

3. Frontal Passage Climatology at the BMC

[15] The oceanic and atmospheric synoptic conditions during expeditions OP23 to OP26 have been analyzed in detail by *Pezzi et al.* [2009]. Here, it is important to characterize each of the experiments relatively to the closest frontal passage (Table 1).

[16] The study area is an extratropical region, influenced by two types of thermal contrasts, one originated by the land-sea temperature differences and the other by the confluence of two oceanic currents. Therefore, the transient pressure systems present a large variability regarding their configuration and intensity. Besides, it is a cyclogenetical and frontogenetical region [*Gan and Rao*, 1991; *Hoskins and Hodges*, 2005]. As a consequence, it is possible to identify a large number of frontal systems passing across the region, allowing the statistical validation of a climatological representation.

[17] A climatology of the frontal passages in the study region was performed for the months of October and November 2004 to 2008. A total of 26 frontal systems were identified subjectively considering pressure tendency, temperature gradient and the maximum cyclonic wind shear obtained from the NCEP reanalysis [*Kalnay et al.*, 1996]. These results are presented in Figure 2. The frontal passage was assumed to occur when the pressure at a representative point in the BMC region (40°S, 55°W) was at a minimum. From that, the averaged daily fields were constructed with respect to the frontal passage day in that particular location (assumed to be day 0). The fields are considered smoothed representations of the real frontal passages, as a consequence of the averaging process applied here.

[18] The averaged synoptic field indicates that, 2 days before the frontal passage (day −2), the semipermanent South Atlantic high is located to the east of the BMC region, driving a northerly large-scale circulation over it, and causing warm advection at the region. A meridionally oriented trough is located at southern Argentina, east of the Andean mountains. Such trough indicates the frontal system that will reach the confluence 2 days later. A transient high is present west of the Andes. The condition observed at the 2006 operation (OP25) resembles the averaged situation of day −2. The high is located to the east of the confluence, and produces warm air advection over the region, in close agreement to the climatological field.

[19] At day −1 the center of the high-pressure system moves eastward, maintaining the positive thermal advection at the study region. The climatological frontal system trough advances slightly in the same direction, determining a saddle point just to the west of the point used as representative for the BMC. The Pacific high pressure starts to cross the Andean mountains. Such characteristics are very similar to those observed during the 2007 campaign (OP26), when the trough is also slightly to the west of the BMC, but the observed wind convergence is larger than the climatological field.

[20] At the frontal passage day (day 0), the center of the South Atlantic high is further east of its original position (day −2) and the frontal trough is located over the BMC. Warm air advection still occurs at the confluence, but with smaller magnitude, as the meridional wind component is decreasing in magnitude. The Pacific high is now causing cold-air advection at southern Argentina. The synoptic conditions for OP23, in 3 November 2004 indicate that the Atlantic high is at a place similar to that of the climatological field, and so does the frontal trough. The reanalysis field presents a well-developed trough, which corresponds to a later stage relatively to the climatological field. The Pacific high causes intense cold advection at southern Argentina, again characteristic of a slightly later stage relatively to the climatology. The low-pressure system located at northern Argentina causes a northerly flow at the BMC, while the Pacific high drives southerlies at the same point, originating local wind convergence.

[21] At the first day after the frontal passage (day +1), the South Atlantic high moves further east, so that only the northerly flow at its western side can be seen in Figures 2a–2e. A subtle anticyclonic flow occurs at central Argentina, as well as over the BMC. The frontal trough advances to the east of the confluence, driving cold-air advection over it. On 14 October 2008, a high-pressure system causes southerly flow at the BMC and the trough-induced flow occurs far away to the east of the confluence.

[22] Finally, at day +2, the climatology shows that the transient high from the Pacific has crossed the Andes, maintaining the anticyclonic flow and cold-air advection over the confluence. Despite being a postfrontal situation, the synoptic chart from 28 October 2005, the day of OP26, is quite different from the climatology. This is a consequence of the variability of the synoptic systems at the region. In this day, a brief cyclogenesis occurs after the passage of a large extratropical cyclone. In Figure 2 (lowest right panel), which represents the daily averaged fields, this can be observed as a low-pressure system just to the east of the confluence. Nevertheless, cold thermal advection occurs at the BMC, caused by its location at the rear of the frontal trough associated to the low pressure. Therefore, despite the very different configuration, in terms of thermal advection this day can be associated to the climatology of day +2.

[23] The thermal advection can be estimated from the directional wind shear [*Bluestein*, 1992], using the average wind and temperature profiles along each cruise. The estimated thermal advection in each case (Table 1) confirms the occurrence of prefrontal conditions during OP25 and OP26 (warm advection) and postfrontal conditions during OP24 and OP27 (cold advection). A weak cold advection is estimated for OP23, and the small magnitude is indicative of the frontal passage during that expedition. Wind hodographs (Figure 3) show counterclockwise turning of the wind with height for the two prefrontal cases, and clockwise turning for the two postfrontal situations. For OP23, assumed as indicative of day 0, almost no wind turning with height is perceivable. Figure 3 also shows that during both OP25 and OP26 the meridional wind component was northerly both

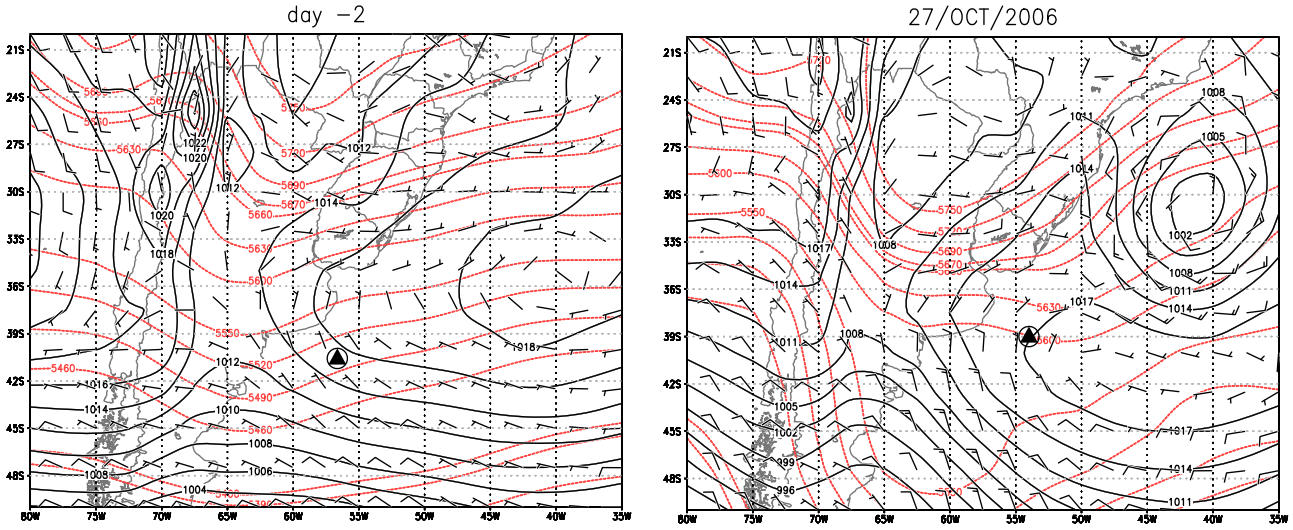

Figure 2a. Average pressure fields (solid lines) and atmospheric thickness between 1000 and 500 HPa levels (dashed lines) for (left) day −2 with respect to the closest frontal passage and (right) 27 October 2006. Black triangles indicate a reference point for the BMC region (40°S, 55°W), for which the minimum sea level pressure is considered for determining frontal passages.

at lower and upper levels and southerly during OP24 and OP27.

4. MABL Structure and Thermal Advection

[24] The analysis presented here focuses on the average boundary layer state over each side of the confluence. This is done because, in all cases, the thermal structure was very similar for profiles taken over a given side, while it is appreciably different between each of the sides. In other words, the profile variability from one side to the other is always larger than over any of the sides. Table 2 shows the virtual potential temperature variability for all the cases and sides.

4.1. Warm Advection

[25] The case of warm advection across a SST gradient has not been observed very frequently. In fact, most of the studies that analyze such situation focus on coastal regions, where the warm, terrestrial air is advected over the colder ocean [*Vickers et al.*, 2001; *Vihma and Brummer*, 2002; *Angevine et al.*, 2006]. In this case, the warm air that flows over the colder surface creates a stable internal boundary layer [*Mahrt et al.*, 2004].

[26] In the present analysis, a well-established warm advection pattern occurred at the BMC during OP25, whose characteristics are similar to those of day +2 of the synoptic cycle, as shown in the previous section. The averaged profiles from OP25 (Figures 4a–4c) show a classical stable boundary

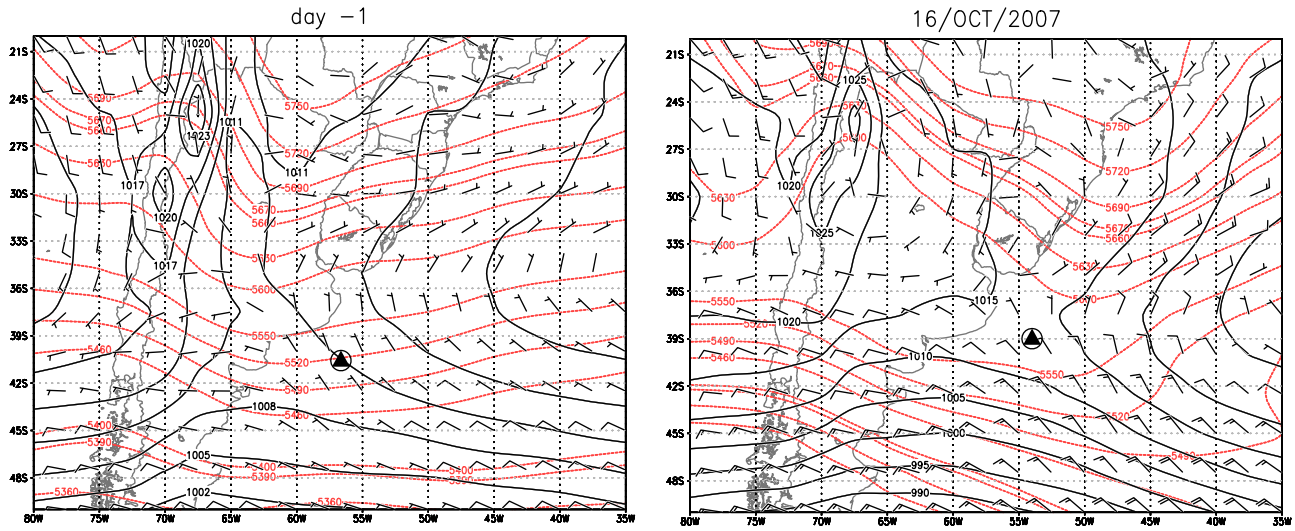

Figure 2b. Same as Figure 2a, but for (left) day −1 and (right) 16 October 2007.

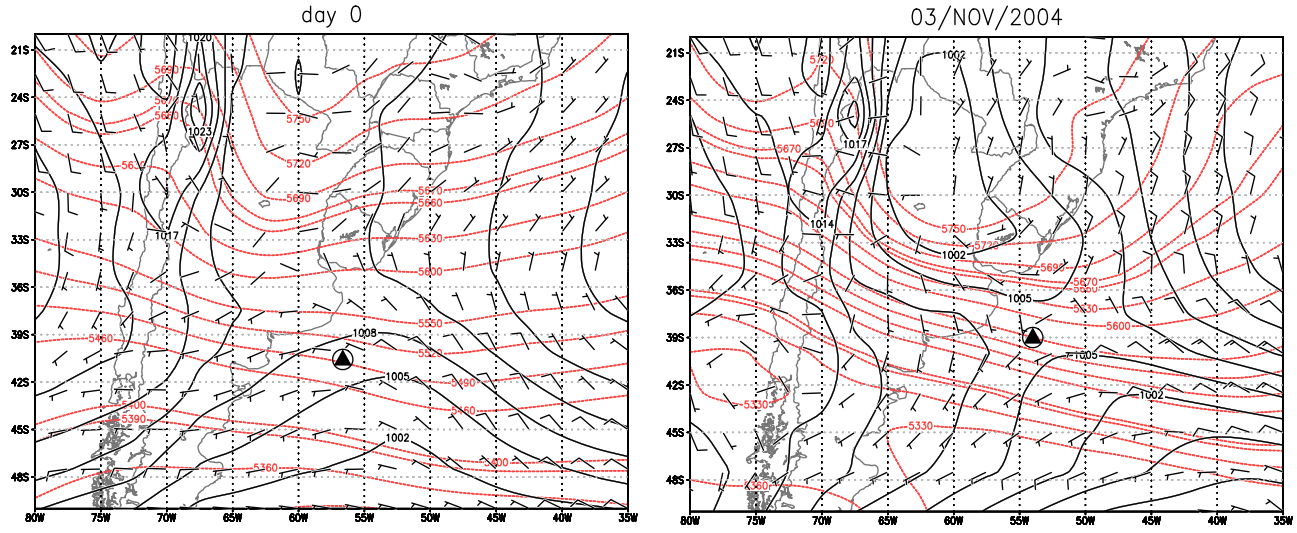

Figure 2c. Same as Figure 2a, but for (left) day 0 and (right) 3 November 2004.

layer vertical structure at the cold region of the BC/MC front. A sharp surface inversion occurs, with the largest stratification occurring within a 200 m layer next to the surface. A local wind maximum is observed at the colder portion, just above the surface highly stable layer. Local wind maxima classified as low-level jets have been observed at the stable boundary layer that forms over the ocean in coastal regions, when warmer air is advected from the continent as a consequence of surface decoupling and acceleration of the air at upper levels [*Smedman et al.*, 1993, 1995; *Vihma and Brummer*, 2002]. The observed profiles of potential temperature and wind magnitude observed in OP25, corresponding to prefrontal conditions, similar to those at day −2, show that both the cold and warm regions are in very close qualitative agreement with the modeling results of *Skyllingstad et al.* [2007] for the case of warm advection. Their results also showed a strongly stratified boundary layer near the surface at the colder region, and a mixed layer at the warmer portion. Furthermore, and similarly to our observations, they found stronger winds at the colder portion, although no local wind maximum over that area occurs in their simulations. The average specific humidity profiles are appreciably different between the warm and cold regions, which show much larger moisture content. Besides, a shallow humidity maximum is observed over the cold region, roughly at the same layer of the highly stable surface stratification and just below the low-level wind maximum as shown in Figure 8 (central lower panel). Previous studies that looked primarily at CO_2 showed that large scalar accumulation is favored below the local wind peak on land above vegetative canopies [*Mathieu et al.*, 2005; *Acevedo et al.*, 2008; *Prabha et al.*, 2008]. The highly stable surface layer, low-level wind maximum and intense scalar accumulation observed in OP25 suggest that a similar process is occurring at the colder side of the BC/MC front when warm air advection occurs. Large moisture accumulation at lower levels above the cold side

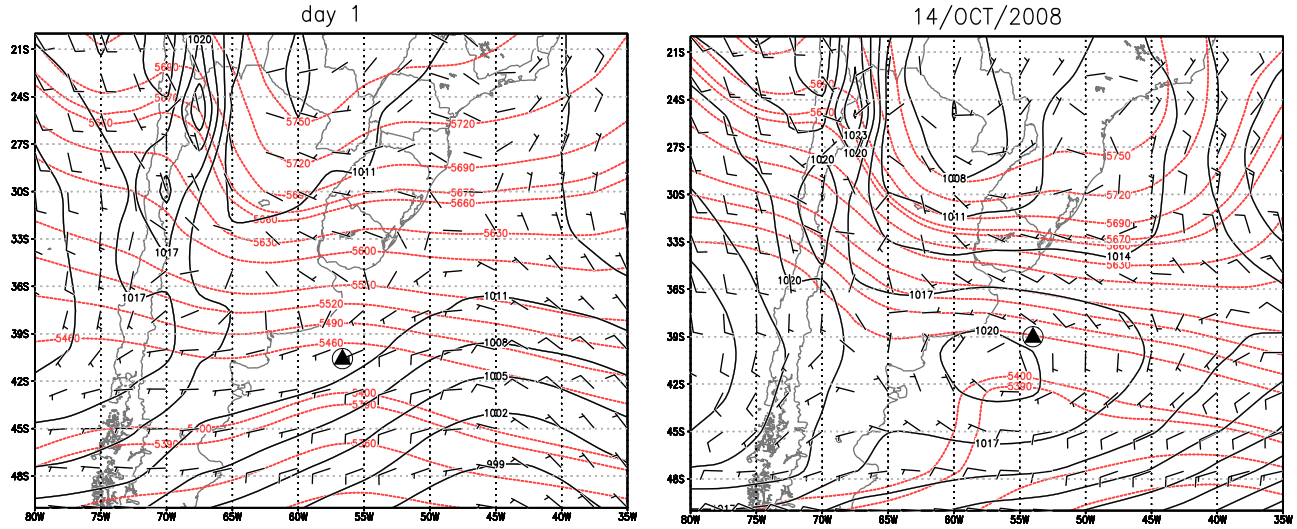

Figure 2d. Same as Figure 2a, but for (left) day +1 and (right) 14 October 2008.

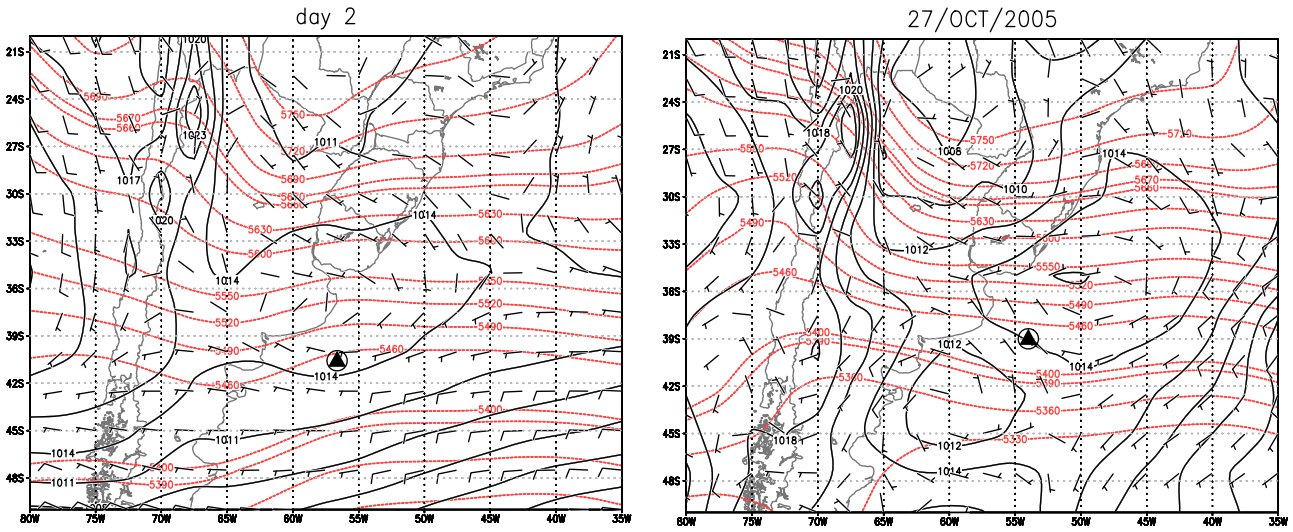

Figure 2e. Same as Figure 2a, but for (left) day +2 and (right) 28 October 2005.

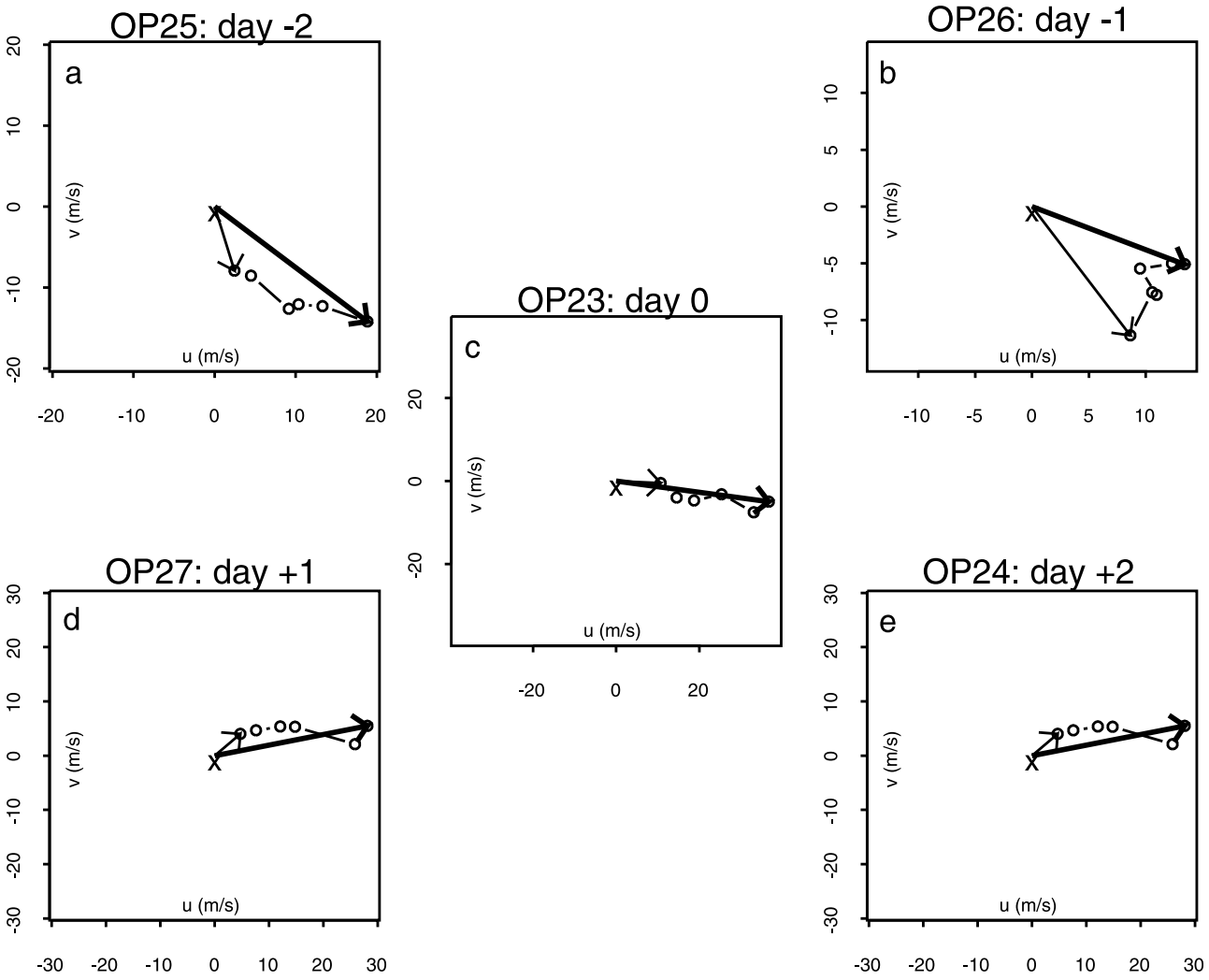

Figure 3. The average observed winds at 1000 m (thin arrows) and 6000 m (thick arrows) for each cruise. The dots indicate the average winds at subsequent levels calculated at 1000 m intervals.

Table 2. Standard Deviation of Virtual Potential Temperature at Four Different Levels Over Each Side of the Confluence for Each Experiment

	OP23		OP24		OP25		OP26		OP27	
Side (Profiles)	Warm (3)	Cold (2)	Warm (5)	Cold (7)	Warm (3)	Cold (6)	Warm (3)	Cold (1)	Warm (4)	Cold (6)
250 (K)	1.62	3.11	1.37	0.67	0.32	0.31	0.15	–	0.36	1.12
500 (K)	3.45	3.38	1.28	0.73	0.29	0.57	0.09	–	0.30	0.58
750 (K)	1.49	3.41	1.50	0.72	0.27	0.78	0.12	–	0.38	0.49
1000 (K)	2.05	3.32	1.89	0.74	0.63	0.81	0.63	–	0.88	0.66

of a surface discontinuity has been previously shown in coastal observations presented by *Vihma and Brummer* [2002] and by *Angevine et al.* [2006].

4.2. Cold Advection

[27] The case with cold advection is more commonly reported in previous studies of the MABL structure across SST gradients. *Pyatt et al.* [2005] and *de Szoeke et al.* [2005] presented results from observations across the cold tongue Inter Tropical Convergence Zone (ITCZ) complex in eastern Pacific. Both studies showed that the advected cold air over the warmer region drives convection downwind of the SST gradients, weakening the atmospheric surface inversion.

[28] Similar results are found in our study (Figures 4d–4f). In fact, the averaged profiles of OP24, obtained during a postfrontal situation characteristic of day −2 of the synoptic cycle, show that the weaker inversion observed at the cold region of the SST front is replaced, at the warmer side, by an internal mixed boundary layer, 700 m thick, capped by a

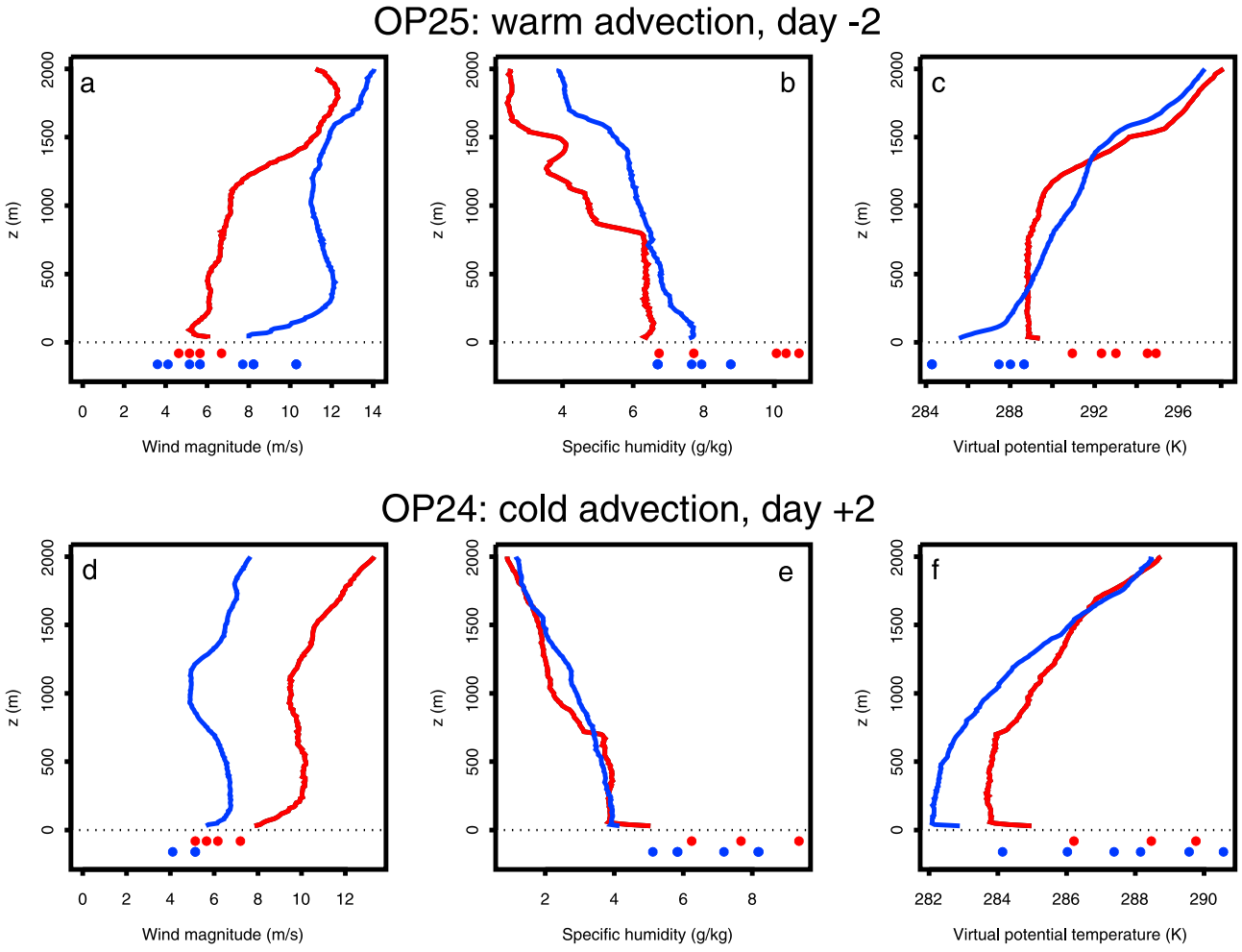

Figure 4. Average vertical profiles of wind magnitude (Figures 4a and 4d), specific humidity (Figures 4b and 4e), and potential temperature (Figures 4c and 4f) for (a–c) OP25 and (d–f) OP24. Red lines represent the average over all soundings made over the warm side, while blue lines represent the average over all soundings made over the cold side. Dots represent the surface conditions, as given by hourly observations made at the ship (red dots for observations at the warm side and blue dots for those at the cold side).

stronger inversion (Figures 4d–4f). Individual profiles show that the mixed layer temperature increases with the distance from the confluence and this fact explains the increased variability over the warm side (Table 2). The blending height, which is the height above the surface where the horizontal heterogeneity effects are no longer perceived, is observed near 1500 m. The humidity profiles are similar between the warm and cold regions, with the remarkable difference that in the warm portion the 700 m capping inversion marks a sharp moisture gradient.

[29] Modeling studies have used large eddy simulation (LES) to study the MABL characteristics when cold advection occurred across a SST gradient. *de Szoeke and Bretherton* [2004] showed a 300 m wind maximum at the cold region, also observed in the present study, and a consequence of surface decoupling from the upper boundary layer, determined by the surface stable stratification. In their simulation, however, the wind maximum over the cold region is stronger than the one observed at OP24 (Figure 4d). Furthermore, our observations show a larger contrast in wind magnitudes between the cold and warm regions. In another LES modeling effort, *Skyllingstad et al.* [2007] simulated the MABL structure over the confluence for both types of thermal advection. For the case of cold advection, their results are in qualitative agreement with our observations, as they show stronger winds in the warmer part of the front, although they did not simulate the cold region wind maximum. Besides, their simulations showed a weaker thermal inversion over the warm portion but not the internal mixed layer observed in OP24 with real data.

4.3. Transitions

[30] In sections 4.1 and 4.2, we described the mean profiles that exist when the cold and warm advection patterns are well established. How is the transition between these states? The profiles taken during the other three cruises provide important information on that.

[31] The well-defined mixed layer observed over the warm side during the warm advection condition originates during the later stages of the cold advection portion of the cycle. In other words, the warm-side mixed layer of OP25 (Figure 4a) is an evolution from something similar to the warm-side mixed layer of OP24 (Figure 4f). Indeed, such a well-defined mixed layer can only occur when there is a heat source from below, which is warranted, in this case, by the warmer waters that exist below the colder air. Once the warm advection condition is established, the forcing for the warm-side mixed layer weakens or disappears. In that case, warmer air blows from lower latitudes toward the BC/MC front, and the consequence is the formation of a slightly stable layer over the warm (BC) side of it, at the region where a mixed layer existed before. At the same time, a more stable layer is sustained by the warm advection at the cold (MC) side. Such situation was observed at OP26, whose characteristics resemble day −1 of the synoptic cycle (Figure 5c). Despite the smaller stability at the lowest 300 m than at the cold side, the MABL at the warm side also presents typical features of a stable boundary layer, such as the local wind maximum (Figure 5a) and the moisture accumulation below it (Figure 5b), both of which are also present at the cold side.

[32] During the transition between warm and cold advection (day 0 of the cycle), convergent winds are observed just above the confluence, and such was the case in OP23. Therefore, the warm advection stabilizes the MABL over the warm side. At this stage, the boundary layer structure over both sides becomes independent of each other (Figures 5d–5f).

[33] Finally, the transition to postfrontal conditions can be seen from the profiles of OP27 (Figure 5g–5i). In such case, a southerly flow happened during the entire cruise, but the vertical profiles are not yet characteristic of a cold advection case. In fact, at the warm side the MABL has characteristics similar to those of OP24, when the cold advection was well-established, with well-mixed potential temperature and specific humidity. However, the MABL at the cold side is still similar to that which occurred during the warm advection, with a stable boundary layer near the surface and a sharp drop in specific humidity above 400 m. Individual profiles show that the lower layer gets more stable as one approaches the confluence, increasing the variability at the lowest levels over the cold side (Table 2). These results, therefore, show that the mixed layer forms quickly at the warm side once the cold advection starts, in this case as a consequence of the sharp contrast between water and air temperatures. However, at the cold side, a longer time is necessary to break the surface layer inversion.

5. Air-Sea Fluxes and MABL Stability

[34] Turbulent sensible and latent heat fluxes represent the variables through which the oceanic masses interact with the atmosphere. Therefore, their adequate determination is crucial to characterize the extent to which the SST gradients of the BC/MC front can affect weather and climatic patterns. Typically, the turbulent fluxes over the ocean are determined by a bulk relationship, through which sensible (latent) heat fluxes are proportional to the temperature (specific humidity) gradient between the air and the sea surface, wind magnitudes and a stability coefficient. The widely used scheme proposed by *Fairall et al.* [1996] was applied here to determine the average turbulent fluxes over each side of the BC/MC front for the five cruises analyzed here (Table 3).

[35] The estimated fluxes show an energy partition dominated by quite large latent heat fluxes from the ocean to the atmosphere at the warm side of the front and at the cold side of it under prefrontal conditions. After the frontal passage, the estimates suggest that the cold side may become a moisture sink, with latent heat fluxes directed from the air to the ocean as seen for OP25, in Table 3. The estimates also indicate that the cold side acts as a sensible heat flux sink at all times, thus removing heat from the atmosphere above it. Latent heat fluxes over the cold side tend to be directed upward, but quite smaller in magnitude than those estimated over the warm side.

[36] These results are consistent with previous studies [e.g., *Chelton et al.*, 2001; *Hashizume et al.*, 2002; *Xie*, 2004; *Tokinaga et al.*, 2005; *Pezzi et al.*, 2005, 2009] which suggested that the atmosphere tends to adjust to the narrow oceanic fronts. MABL goes in a vertical stratification transition from unstable condition over warmer waters to a stable condition over cold waters. This will result on stronger sur-

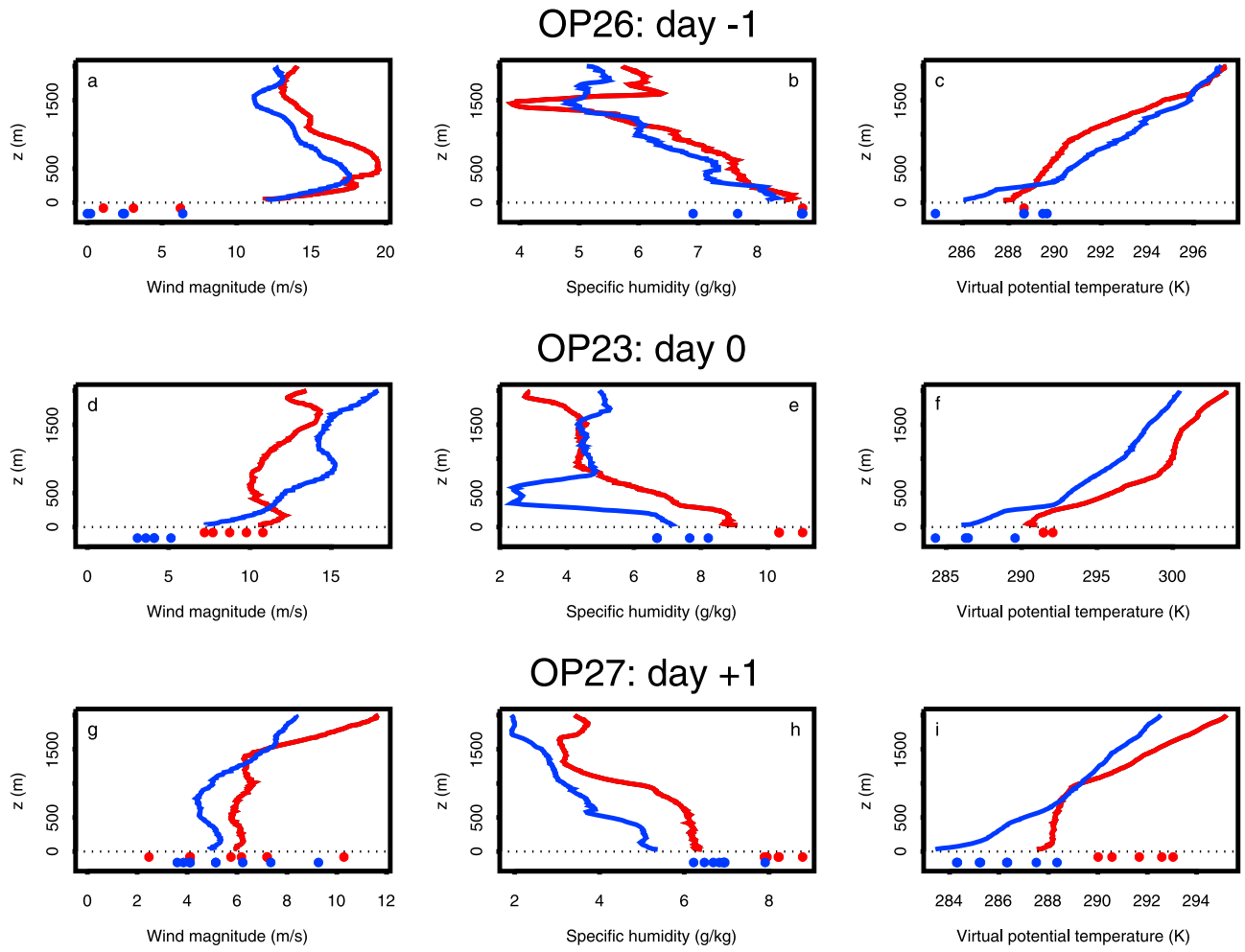

Figure 5. Same as in Figure 4, but for (a–c) OP26, (d–f) OP23, and (e–i) OP27.

face winds over the warmer side of the front while weaker winds will occur over the cold side of it. *Tokinaga et al.* [2005] have analyzed high-resolution annual mean surface wind climatology and it is important to note that (contrary to their results) our in situ observations show a clear signal of the SST effects on the surface winds, modulating the horizontal pressure gradient as already reported in the work of *Pezzi et al.* [2009]. In *Tokinaga et al.*'s [2005] results, the SST frontal effect on the annual mean scalar wind speed is unclear.

[37] How robust are these estimates, considering that the scheme used was proposed for the tropical ocean? Can the vertical profiles presented here provide additional evidence for that purpose?

[38] Sensible heat flux estimates are in general qualitative agreement with the profile evidence. At the warm side of the BC/MC front, our estimated data resulted in upward fluxes for all cases except OP26, when the warm air advection was established for more than 1 day. That brought warmer air from lower latitudes promoting the development of a stable boundary layer at the warm side which drives sensible heat fluxes to be directed from the atmosphere to the ocean. On all other cases, the observed mixed layer at the warm side agrees qualitatively with the estimates. At the cold side, however, the sensible heat flux was estimated as negative (or absent) for all cruises, and this is in qualitative agreement with the stable thermal stratification observed in the MABL potential temperature profiles.

[39] Looking at the latent heat fluxes, however, there are cases when the estimated fluxes seem to contradict the observational evidence from the specific humidity profiles. Considering that we are analyzing a region where latent heat fluxes tend to be appreciably larger than the sensible ones, such discrepancy may have serious implications. Such is the case at the cold side of the front, where the latent heat flux

Table 3. Sensible and Latent Heat Fluxes[a]

Cruise	Day	H Warm (W m^{-2})	LE Warm (W m^{-2})	H Cold (W m^{-2})	LE Cold (W m^{-2})
OP25	−2	21.8 ± 13.3	196.6 ± 33.6	−48.7 ± 9.7	−15.2 ± 17.1
OP26	−1	−3.5 ± 5.7	77.7 ± 46.5	−9.2 ± 16.0	5.9 ± 20.4
OP23	0	18.9 ± 27.0	79.5 ± 31.7	−1.2 ± 6.0	16.6 ± 12.2
OP27	+1	5.8 ± 19.4	152.3 ± 75.1	2.1 ± 40.0	44.2 ± 37.8
OP24	+2	33.1 ± 13.0	174.3 ± 54.9	−9.4 ± 16.5	56.9 ± 37.7

[a]All quantities are averaged along the cruise route over the BC and MC portions of the BMC region. The quantities are denoted as warm and cold referring to calculations made over the BC and the MC, respectively.

estimates are negative for OP25 and appreciably small in both OP23 and OP26. The vertical specific humidity profiles, however, indicated large moisture accumulation near the surface for these cases (Figures 3 and 4), and especially large for OP25. Therefore, appreciable upward latent heat fluxes happen at the cold side of the BC/MC front when warm air advection occurs, but these fluxes are not properly approximated by a bulk parameterization. We believe that this is a consequence of the inadequacy of such schemes for the determination of the surface fluxes within the strongly stratified environment that characterizes the cold portion of the BC/MC front in such situations. In fact, flux measurements made in these conditions support this conclusion. For instance, *Angevine et al.* [2006] reported that the heat flux correlates well with wind speed, but not with the temperature difference. This difficulty in estimating the fluxes is stated by *Vickers et al.* [2001], who argue that "…in regions of significant surface heterogeneity, (…), a well-defined surface layer may not exist, and similarity theory will be inadequate due to a dependence of the fluxes on upstream conditions.."

6. Conclusion

[40] The marine atmospheric boundary layer adjustment to the surface heterogeneity imposed by the intense SST gradients of distinct water masses at the Brazil-Malvinas Confluence region follows a well-defined cycle. Warm and cold air advection, characteristic of prefrontal and postfrontal conditions, respectively, induce large differences on the thermodynamic and dynamic structure of the atmosphere at both (warm and cold) sides of the confluence. Besides that, transitional conditions also have their own, peculiar characteristics as a consequence of shorter relaxation times over a region dominated by shear-generated turbulence [*Moeng and Sullivan*, 1994]. Turbulent heat fluxes over the region are also modulated by both the SST gradients and the synoptic cycle of the region. In many phases of the cycle, a strongly stratified boundary layer occurs at the cold side, or even at the warm side (day −1, Figure 5a). As a consequence of this, the schemes commonly used to estimate heat fluxes tend to fail.

[41] Meteorologists working in southeastern South America frequently observe that numerical weather forecast models tend to underestimate moisture content, especially at postfrontal conditions when the airflows from the oceanic portions near the BMC. In such case, clear sky conditions may be predicted when overcast or even rainy situations actually occur. We believe that the inadequacy of latent heat flux representations at the BMC region is the most important responsible for these discrepancies. *Russo* [2009] showed that numerical weather simulations are sensitive to the inclusion of the observed data at the BMC region by means of radiosonde data assimilation. When comparing (in situ) observed profiles of relative humidity and (zonal, meridional) wind components of the MABL with simulated profiles, *Russo* [2009] found that using the assimilation method the MABL is better represented than when no assimilation is used.

[42] The present study represents a key contribution toward a better understanding of the surface processes occurring at the BMC region. In the future, this knowledge can be used to improve turbulent fluxes representation in the models and, as a consequence, the forecast quality. Before that can be possible, however, it is necessary to quantify the fluxes with higher accuracy than is nowadays possible with the available parameterization schemes. To address that issue, in situ flux measurements using the eddy covariance method are planned to be performed in the following field campaigns.

[43] It is also important to say that the higher latitudes of the South Atlantic Ocean are acknowledged as one of the most important carbon sinking regions of the World Ocean [*Takahashi et al.*, 2009; *Bianchi et al.*, 2009]. Our future knowledge on the annual balance and variability of the CO_2 fluxes between the ocean and the atmosphere along the Subtropical Front and on the Southwestern Atlantic Ocean is dependent on a better understanding of the local variability of the water masses, phytoplankton concentration and turbulent fluxes at the ocean-atmosphere interface.

[44] **Acknowledgments.** We thank Paulo Arlino and the Meteorological Instrumentation Laboratory of CPTEC-INPE for the support for the field campaigns. Ernani L. Nascimento provided valuable suggestions on the wind direction analysis. The Brazilian Navy and the captain and crew of the OSS *Ary Rongel* are acknowledged for their help in the planning and execution of all cruises. Radiosondes and XBTs were provided by CPTEC-INPE, INMET, SOS-Climate project, and AOML/NOAA. We also thank CNPq-PROANTAR, CIRM, FAPESP, and the Brazilian Ministry of the Environment. The research was funded by projects 550370/2002–1 (GOAL), 557284/2005–8 (INTERCONF), 2005/02359–0 (OCAT-BM), 520189/2006–0 (SOS-CLIMATE), 704222/2009 (INCT Cryosphere), and 558108/2009–1 (ACEx). O.C.A. and G.A.D. acknowledge support from CNPq. L.P.P. was also supported by CNPq projects 306670/2006–2 and 476971/2007–1.

References

Acevedo, O. C., R. Silva, D. R. Fitzjarrald, O. L. L. Moraes, R. K. Sakai, and M. J. Czikowski (2008), Nocturnal vertical CO_2 accumulation in two Amazonian ecosystems, *J. Geophys. Res.*, *113*, G00B04, doi:10.1029/2007JG000612.

Angevine, W. M., J. E. Hare, C. W. Fairall, D. E. Wolfe, R. J. Hill, W. A. Brewer, and A. B. White (2006), Structure and formation of the highly stable marine boundary layer over the Gulf of Maine, *J. Geophys. Res.*, *111*, D23S22, doi:10.1029/2006JD007465.

Bianchi, A. A., D. R. P. Hernan, G. I. Perlender, A. P. Osiroff, V. Segura, V. Lutz, M. L. Clara, C. F. Balestrini, and A. R. Piola (2009), Annual balance and seasonal variability of sea-air CO2 fluxes in the Patagonia Sea: Their relationship with fronts and chlorophyll distribution, *J. Geophys. Res.*, *114*, C03018, doi:10.1029/2008JC004854.

Bluestein, H. B. (1992), *Synoptic-Dynamic Meteorology in Midlatitudes*, 431 pp., Oxford Univ. Press, New York.

Chelton, D. B., M. G. Schlax, D. L. Witter, and J. G. Richman (1990), GEOSAT altimeter observations of the surface circulation of the Southern Ocean, *J. Geophys. Res.*, *95*, 17,877–17,903, doi:10.1029/JC095iC10p17877.

Chelton, D. B., S. K. Esbensen, M. G. Schlax, N. Thun, M. Freilich, F. J. Wentz, C. L. Gentmann, M. J. McPhaden, and P. S. Schopf (2001), Observations of coupling between surface wind stress and sea surface temperature in the eastern tropical pacific, *J. Clim.*, *14*, 1479–1498, doi:10.1175/1520-0442(2001)014<1479:OOCBSW>2.0.CO;2.

Deacon, G. E. R. (1937), The hydrology of the Southern Ocean, *Discovery Rep.*, *15*, 3–122.

de Szoeke, S. P., and C. S. Bretherton (2004), Quasi-Lagrangian large eddy simulation of cross-equatorial flow in the east Pacific atmospheric boundary layer, *J. Atmos. Sci.*, *61*, 1837–1858, doi:10.1175/1520-0469(2004)061<1837:QLESOC>2.0.CO;2.

de Szoeke, S. P., C. S. Bretherton, N. A. Bond, M. F. Cronin, and B. M. Morley (2005), EPIC 95°W observations of the eastern Pacific atmospheric boundary layer from the cold tongue to the ITCZ, *J. Atmos. Sci.*, *62*, 426–442, doi:10.1175/JAS-3381.1.

Fairall, C. W., E. F. Bradley, D. P. Rogers, J. B. Edson, and G. S. Young (1996), Parameterization of air-sea fluxes for Tropical Ocean-Global Atmosphere Coupled-Ocean Atmosphere Response Experiment, *J. Geophys. Res.*, *101*, 3747–3764, doi:10.1029/95JC03205.

Gan, M. A., and V. B. Rao (1991), Surface cyclogenesis over South America, *Mon. Weather Rev.*, *119*, 1293–1302, doi:10.1175/1520-0493(1991)119<1293:SCOSA>2.0.CO;2.

Garzoli, S., and Z. Garraffo (1989), Transports, frontal motions and eddies at the Brazil-Malvinas Currents Confluence, *Deep Sea Res.*, *36*, 681–703, doi:10.1016/0198-0149(89)90145-3.

Hashizume, H., S.-P. Xie, M. Fujiwara, M. Shiotani, T. Watanabe, Y. Tanimoto, W. T. Liu, and K. Takeuchi (2002), Direct observations of atmospheric boundary layer response to SST variations associated with tropical instability waves over the eastern equatorial Pacific, *J. Clim.*, *15*, 3379–3393, doi:10.1175/1520-0442(2002)015<3379:DOOABL>2.0.CO;2.

Hayes, S. P., M. J. McPhaden, and J. M. Wallace (1989), The influence of sea surface temperature on surface wind in the eastern equatorial Pacific: Weekly to monthly variability, *J. Clim.*, *2*, 1500–1506, doi:10.1175/1520-0442(1989)002<1500:TIOSST>2.0.CO;2.

Hoskins, B. J., and K. I. Hodges (2005), A new perspective on Southern Hemisphere storm tracks, *J. Clim.*, *18*, 4108–4129, doi:10.1175/JCLI3570.1.

Kalnay, E., et al. (1996), The NCEP/NCAR 40-year reanalysis project, *Bull. Am. Meteorol. Soc.*, *77*, 437–470, doi:10.1175/1520-0477(1996)077<0437:TNYRP>2.0.CO;2.

Legeckis, R., and A. L. Gordon (1982), Satellite observations of the Brazil and Falkland Currents—1975 to 1976 and 1978, *Deep Sea Res.*, *29*, 375–401, doi:10.1016/0198-0149(82)90101-7.

Lindzen, R. S., and S. Nigam (1987), On the role of sea surface temperature gradients in forcing low-level winds and convergence in the tropics, *J. Atmos. Sci.*, *44*, 2418–2436, doi:10.1175/1520-0469(1987)044<2418:OTROSS>2.0.CO;2.

Mahrt, L., D. Vickers, and E. Moore (2004), Flow adjustments across sea-surface temperature changes, *Boundary Layer Meteorol.*, *111*, 553–564, doi:10.1023/B:BOUN.0000016600.63382.5f.

Mathieu, N., I. B. Strachan, M. Y. Leclerc, A. Karipot, and E. Pattey (2005), Role of low-level jets and boundary-layer properties on the NBL budget technique, *Agric. For. Meteorol.*, *135*, 35–43, doi:10.1016/j.agrformet.2005.10.001.

Moeng, C.-H., and P. P. Sullivan (1994), A comparison of shear- and buoyancy-driven planetary boundary layer flows, *J. Atmos. Sci.*, *51*, 999–1022, doi:10.1175/1520-0469(1994)051<0999:ACOSAB>2.0.CO;2.

Olson, D. B., G. P. Podestá, R. H. Evans, and O. B. Brown (1988), Temporal variations in the separation of Brazil and Malvinas currents, *Deep Sea Res.*, *35*, 1971–1990.

Peterson, R. G., and L. Stramma (1991), Upper-level circulation in the South Atlantic Ocean, *Prog. Oceanogr.*, *26*, 1–73, doi:10.1016/0079-6611(91)90006-8.

Pezzi, L. P., J. Vialard, K. J. Richards, C. Menkes, and D. Anderson (2004), Influence of ocean-atmosphere coupling on the properties of tropical instability waves, *Geophys. Res. Lett.*, *31*, L16306, doi:10.1029/2004GL019995.

Pezzi, L. P., R. B. Souza, M. S. Dourado, C. A. E. Garcia, M. M. Mata, and M. A. F. Silva Dias (2005), Ocean-atmosphere in-situ observations at the Brazil-Malvinas confluence region, *Geophys. Res. Lett.*, *32*, L22603, doi:10.1029/2005GL023866.

Pezzi, L. P., R. B. de Souza, O. Acevedo, I. Wainer, M. M. Mata, C. A. E. Garcia, and R. de Camargo (2009), Multiyear measurements of the oceanic and atmospheric boundary layers at the Brazil-Malvinas confluence region, *J. Geophys. Res.*, *114*, D19103, doi:10.1029/2008JD011379.

Piola, A. R., and R. P. Matano (2001), Brazil and Falklands (Malvinas) currents, in *Encyclopedia of Ocean Sciences*, edited by S. A. Thorpe, pp. 340–349, Elsevier, New York.

Polito, P., J. P. Ryan, W. T. Liu, and F. P. Chavez (2001), Oceanic atmospheric anomalies of tropical instability waves, *Geophys. Res. Lett.*, *28*, 2233–2236, doi:10.1029/2000GL012400.

Prabha, T. V., M. Y. Leclerc, A. Karipot, D. Y. Hollinger, and E. Mursch-Radlgruber (2008), Influence of nocturnal low-level jets on eddy-covariance fluxes over a tall forest canopy, *Boundary Layer Meteorol.*, *126*, 219–236, doi:10.1007/s10546-007-9232-3.

Pyatt, H. E., B. A. Albrecht, C. Fairall, J. E. Hare, N. Bond, P. Minnis, and J. K. Ayers (2005), Evolution of marine atmospheric boundary layer structure across the Cold Tongue-ITCZ Complex, *J. Clim.*, *18*, 737–753, doi:10.1175/JCLI-3287.1.

Reid, J. L., W. D. Nowlin Jr., and W. C. Patzerd (1977), On the characteristics and circulation of the southwestern Atlantic Ocean, *J. Phys. Oceanogr.*, *7*, 62–91, doi:10.1175/1520-0485(1977)007<0062:OTCACO>2.0.CO;2.

Russo, L. (2009), Ocean-atmosphere interaction at the southwestern Atlantic Ocean in the Brazil-Malvinas Confluence Region (in Portuguese), M.S. dissertation, Natl. Inst. for Space Res., São José dos Campos, Sao Paulo, Brazil.

Skyllingstad, E. D., D. Vickers, L. Mahrt, and R. Samelson (2007), Effects of mesoscale sea-surface temperature fronts on the marine atmospheric boundary layer, *Boundary Layer Meteorol.*, *123*, 219–237, doi:10.1007/s10546-006-9127-8.

Small, R. J., S. P. de Szoeke, S. P. Xie, L. O'Neill, H. Seo, Q. Song, P. Cornillon, M. Spall, and S. Minobe (2008), Air–sea interaction over ocean fronts and eddies, *Dyn. Atmos. Oceans*, *45*, 274–319, doi:10.1016/j.dynatmoce.2008.01.001.

Smedman, A.-S., M. Tjernstrom, and U. Hogstrom (1993), Analysis of the turbulence structure of a marine low-level jet, *Boundary Layer Meteorol.*, *66*, 105–126, doi:10.1007/BF00705462.

Smedman, A.-S., H. Bergstrom, and U. Hogstrom (1995), Spectra, variances and length scales in a marine stable boundary layer dominated by a low level jet, *Boundary Layer Meteorol.*, *76*, 211–232, doi:10.1007/BF00709352.

Souza, R. B., M. M. Mata, C. A. E. Garcia, M. Kampel, E. N. Oliveira, and J. A. Lorenzzetti (2006), Multi-sensor satellite and in situ measurements of a warm core eddy south of the Brazil-Malvinas Confluence region, *Remote Sens. Environ.*, *100*, 52–66, doi:10.1016/j.rse.2005.09.018.

Takahashi, T., et al. (2009), Climatological mean and decadal change in surface ocean pCO_2, and net sea–air CO_2 flux over the global oceans, *Deep Sea Res., Part II*, *56*, 554–577, doi:10.1016/j.dsr2.2008.12.009.

Tokinaga, H., Y. Tanimoto, and S.-P. Xie (2005), SST-induced wind variations over Brazil-Malvinas confluence: Satellite and in situ observations, *J. Clim.*, *18*, 3470–3482, doi:10.1175/JCLI3485.1.

Vickers, D., L. Mahrt, J. Sun, and T. Crawford (2001), Structure of offshore flow, *Mon. Weather Rev.*, *129*, 1251–1258, doi:10.1175/1520-0493(2001)129<1251:SOOF>2.0.CO;2.

Vihma, T., and B. Brummer (2002), Observations and modeling of the on-ice and off-ice air flow over the northern Baltic Sea, *Boundary Layer Meteorol.*, *103*, 1–27, doi:10.1023/A:1014566530774.

Xie, S. P. (2004), Satellite observations of cool ocean-atmosphere interaction, *Bull. Am. Meteorol. Soc.*, *85*, 195–208, doi:10.1175(BAMS-82–2-195).

O. C. Acevedo, V. Anabor, and G. A. Degrazia, Department of Physics, Federal University of Santa Maria, Santa Maria, RS 97105-900, Brazil. (otavio@smail.ufsm.br)

L. P. Pezzi, Earth Observation General Coordination, National Institute for Space Research, São José dos Campos, SP 12227-010, Brazil.

R. B. Souza, Southern Regional Center for Space Research, National Institute for Space Research, Santa Maria, RS 97105-970, Brazil.